

Reaction of 1,3-diols with $\text{Al}(\text{tBu})_3$ and $\text{Ga}(\text{tBu})_3$: aluminium- and gallium-based bifunctional tetradentate ligands

C. Niamh McMahon,^a Stephen J. Obrey,^a Andrea Keys,^a Simon G. Bott^{*b} and Andrew R. Barron^{*a}

^a Department of Chemistry, Rice University, Houston, Texas 77005, USA.

E-mail: arb@rice.edu

^b Department of Chemistry, University of Houston, Houston, Texas 77204, USA.

E-mail: sbott@bayou.uh.edu

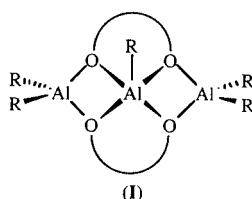
Received 13th January 2000, Accepted 24th April 2000

Published on the Web 8th June 2000

Reaction of $\text{M}(\text{tBu})_3$ ($\text{M} = \text{Al}, \text{Ga}$) with neol- H_2 (2,2-dimethylpropane-1,3-diol) yields $[\text{M}_2(\text{tBu})_4(\text{neol-H})_2]$, $\text{M} = \text{Al}$ (**1**) and Ga (**2**), respectively. Use of an equimolar mixture of $\text{Al}(\text{tBu})_3$ and $\text{Ga}(\text{tBu})_3$ allows for the formation of $[\text{AlGa}(\text{tBu})_4(\text{neol-H})_2]$ (**3**). Compounds **1** and **2** may be considered as bifunctional (two OH groups), tetradentate (4O) ligands as highlighted by their reactivity with Group 13 hydrides and alkyls. Reaction of compound **1** with $\text{AlH}_3(\text{NMe}_3)$, $\text{AlH}_2\text{Cl}(\text{NMe}_3)$ and AlMe_3 yields the tri-aluminium compounds, $[\text{Al}_3(\text{tBu})_4(\text{X})(\text{neol})_2]$ with $\text{X} = \text{H}$ (**4**), $\text{X} = \text{Cl}$ (**5**), Me (**6**), respectively. Similarly, compound **2** reacts with $\text{Ga}(\text{tBu})_3$ to yield the tri-gallium compound, $[\text{Ga}_3(\text{tBu})_5(\text{neol})_2]$ (**7**). The mixed metal complexes, $[\text{Ga}_2\text{Al}(\text{tBu})_4(\text{X})(\text{neol})_2]$, where $\text{X} = \text{H}$ (**8**), Me (**9**) and tBu (**10**), are formed by the reaction of compound **2** with $\text{AlH}_3(\text{NMe}_3)$, AlMe_3 , and $\text{Al}(\text{tBu})_3$, respectively. The solid state conformation of the neol backbone and the ^1H NMR chemical shift of the neol's CH_2 protons, in compounds **4–10**, are both dependent on the steric bulk of the substituent of the central metal. Thermolysis of compound **2** in toluene results in the formation of $[\text{Ga}_3(\text{tBu})_4(\text{CH}_2\text{Ph})(\text{neol})_2]$ (**11**), while the reaction of **2** with LiOH in Et_2O and hexane yields $[\text{Ga}_3\text{Li}_4(\text{tBu})_6(\text{neol})_3(\text{OH})(\text{THF})]$ (**12**) and $[\text{Ga}_2\text{Li}(\text{tBu})_4(\text{OH})_2(\text{neol-H})]$ (**13**), respectively. The molecular structures of compounds **1**, **2**, **4–13** and $[\text{Ga}_3\text{Cl}_5(\text{OSiMe}_2\text{OSiMe}_2\text{O}_2)]$ (**14**) have been determined by X-ray crystallography.

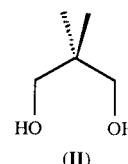
Introduction

The structures of trimetallic compounds of aluminium mainly fall into two general categories.¹ The first is typified by the dialkylaluminium alkoxides in which the alkoxide and alkyl ligands are sterically undemanding, e.g., $[\text{Me}_2\text{Al}(\mu\text{-OMe})_3]$.² The second may be categorized as a “linear” trimer, in which the terminal aluminium centers are four coordinate and the central aluminium is five coordinate. The simplest examples of this latter group are the penta-alkyl trialuminium compounds formed from the reaction of trialkylaluminium with aliphatic diols (**I**),^{3–5} however, an increasing number of these compounds



have been reported with the salen class of N_2O_2 tetradentate ligands.⁵

We have recently reported the reaction of $\text{Al}(\text{tBu})_3$ with ethylene glycol as a route to alucone polymers (aluminium alkoxide materials with carbon-containing backbones).⁶ As an extension of those studies we have now investigated the effects of increasing the length of the diol backbone through the reaction of $\text{Al}(\text{tBu})_3$ and $\text{Ga}(\text{tBu})_3$ with 2,2-dimethylpropane-1,3-diol (neol- H_2 , **II**). We note that Ziemkowska and Pasynkiewicz have previously reported that the reaction of neol- H_2 with AlMe_3 yielded the trimetallic compound, $[\text{Al}_3\text{Me}_3(\text{neol})_2]$.⁴



Results and discussion

Reaction of $\text{M}(\text{tBu})_3$ with neol- H_2

The reaction of $\text{M}(\text{tBu})_3$ ($\text{M} = \text{Al}, \text{Ga}$) with neol- H_2 yields the colorless solid $[\text{M}_2(\text{tBu})_4(\text{neol-H})_2]$, $\text{M} = \text{Al}$ (**1**) and Ga (**2**), respectively. Compound **1** is the only product isolated irrespective of the $\text{Al}(\text{tBu})_3$:neol- H_2 ratio which ranged from 1:1 to 4:1. The reaction of an equimolar mixture of $\text{Al}(\text{tBu})_3$ and $\text{Ga}(\text{tBu})_3$ with neol- H_2 results in a mixture of compounds **1**, **2** and the mixed metal compound, $[\text{AlGa}(\text{tBu})_4(\text{neol-H})_2]$ (**3**) (3.7%) and a trimetallic species (see below).

The NMR spectroscopy and mass spectrometry of compounds **1–3** are consistent with their formulation, see Experimental section. The molecular structures of compounds **1** and **2** have been determined by X-ray crystallography and are shown in Fig. 1 and 2, respectively; selected bond lengths and angles are given in Table 1. Both structures consist of $\text{M}_2\text{O}_4\text{C}_6$ 12-membered cycles with the oxygen atoms endocyclic. Bond lengths about both aluminium and gallium are in the ranges expected.⁷

We were unable to locate the neols' alcohol protons in the difference map of compound **1**, however, their presence is confirmed by ^1H NMR spectroscopy. The neol alcohol protons in compounds **1** and **2** are significantly shifted downfield (δ 16.16

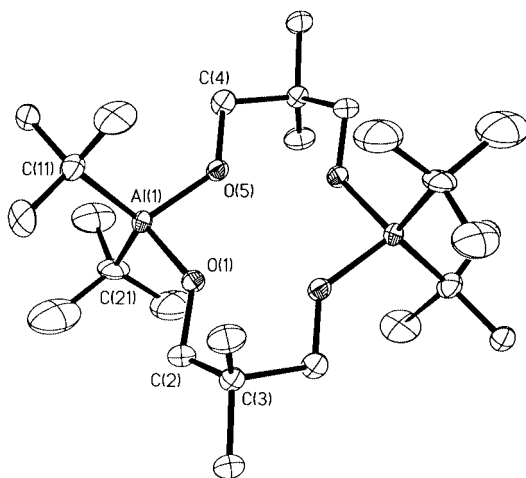


Fig. 1 Molecular structure of $[\text{Al}_2(\text{tBu})_4(\text{neol-H})_2]$ (**1**). Thermal ellipsoids are shown at the 30% level, and all hydrogens are omitted for clarity.

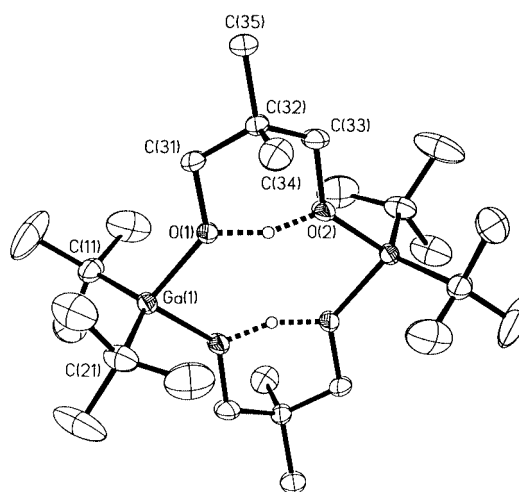
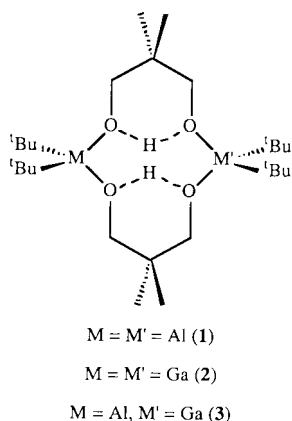


Fig. 2 Molecular structure of $[\text{Ga}_2(\text{tBu})_4(\text{neol-H})_2]$ (**2**). Thermal ellipsoids are shown at the 30% level, and all hydrogens are omitted for clarity.

Table 1 Selected bond lengths (Å) and angles (°) in $[\text{M}_2(\text{tBu})_2(\text{neol-H})_2]$, $\text{M} = \text{Al}$ (**1**), Ga (**2**)

	[Al ₂ (^t Bu) ₂ - (neol-H) ₂] (1)		[Ga ₂ (^t Bu) ₂ - (neol-H) ₂] (2)
Al(1)–O(1)	1.809(3)	Ga(1)–O(1)	1.932(3)
Al(1)–O(5)	1.813(3)	Ga(1)–O(2)	1.930(3)
Al(1)–C(11)	1.975(6)	Ga(1)–C(11)	1.988(6)
Al(1)–C(21)	1.985(7)	Ga(1)–C(21)	1.989(5)
O(1)–Al(1)–O(5')	92.8(1)	O(1)–Ga(1)–O(2')	89.6(1)
C(11)–Al(1)–C(21)	121.7(2)	C(11)–Ga(1)–C(21)	128.5(3)
Al(1)–O(1)–C(2)	133.2(2)	Ga(1)–O(1)–C(31)	129.7(3)
O(1)–C(2)–C(3)	111.6(4)	O(1)–C(31)–C(32)	111.1(4)
C(2)–C(3)–C(4)	108.4(4)	C(31)–C(32)–C(33)	108.2(4)
C(3)–C(4)–O(5)	110.0(3)	C(32)–C(33)–O(2)	109.9(4)
C(4)–O(5)–Al(1')	132.0(2)	C(33)–O(1)–Ga(1')	129.5(3)

and 15.01, respectively) from those in neol- H_2 (δ 2.17), consistent with increased acidity. Complexation of alcohols to aluminium has been shown previously to increase the acidity of the alcoholic proton.⁸ The ^1H NMR signals for the O–H protons in compounds **1** and **2** are narrow ($W_{1/2} \approx 1$ Hz) indicative of no dynamic exchange, while the lack of a $\nu_{\text{O-H}}$ band in the IR spectra for compounds **1** and **2** suggests a strong hydrogen bonding interaction. We propose that the alcohol's hydrogen is involved in strong symmetrical intra-ligand hydrogen bonding between O(1) and O(5). Consistent with this proposal is the magnetic equivalence of the methylene groups in the ^1H and ^{13}C NMR spectra, see Experimental section. Thus, the neol-H ligands are constrained by hydrogen bonding to form two 6-membered rings joined by the two $\text{M}(\text{tBu})_2$ moieties. Examination of the CSD database indicated no previously characterized dimers containing bridging alcohol–alkoxide species and the only 6-membered $\text{O}=\text{C}-\text{C}-\text{O}-\text{H}$ cycles are enol–carbonyl or carboxylate–carbonyl species.⁹

As may be clearly seen from Fig. 3a, the quaternary carbon of the neol-H ring [C(3)] is displaced from the planar arrangement of the remaining atoms of the 6-membered $\text{O}=\text{C}-\text{C}-\text{O}-\text{H}$ cycles. As a result the methyl groups [C(31) and C(32)] adopt axial and equatorial positions. As a consequence of the molecules crystallographic center of symmetry, the overall geometry of compounds **1** and **2** is a chair-like conformation, see Fig. 3a. Based upon ^1H and ^{13}C NMR spectroscopy of compounds **1** and **2** (see Experimental section) it is clear that this conformation is not rigid in solution, since the *tert*-butyl ligands on each metal, the methyl substituents on neol-H ligands and the CH_2 groups of the neol ring each show magnetic equivalence implying an overall planar symmetry for compounds **1** and **2** in solution. This would be observed if

inversion of the chair-like conformation was occurring faster than the NMR experiment time-scale.

Reaction of $[\text{M}_2(\text{tBu})_4(\text{neol-H})_2]$ with MX_3 and $\text{M}'\text{X}_3$

As noted in the Introduction, the tri-aluminium compound, $[\text{Al}_3\text{Me}_3(\text{neol})_2]$ has been previously isolated from the direct reaction of excess AlMe_3 with neol- H_2 .⁴ Although not reported it is probable that the methyl analog of compound **1** was formed as an intermediate. Thus it should be possible to form similar trimetallic species by reacting $[\text{M}_2(\text{tBu})_4(\text{neol-H})_2]$ with MR_3 . Two equivalents of alkane would be eliminated when the trialkyl reacts with the two acidic protons of the dimer. The isolation of compounds **1** and **2** should provide a facile route to both trimetallic species with a different substituent on the central metal atom, *i.e.*, $[\text{M}_3\text{R}_4\text{R}'(\text{neol})_2]$, or a different central metal, *i.e.*, $[\text{M}_2\text{M}'\text{R}_5(\text{neol})_2]$, or a combination of both. Compounds **1** and **2** may be considered as bifunctional (two OH groups), tetradentate (4O) ligands.¹⁰ In this regard they should have chemistry similar to Schiff base ligands and may be thought of as analogs.^{3–5}

The tri-aluminium compounds, $[\text{Al}_3(\text{tBu})_4(\text{X})(\text{neol})_2]$, were readily prepared from the reaction of compound **1** with the appropriate aluminium hydride or alkyl. Reaction of compound **1** with $\text{AlH}_3(\text{NMe}_3)$ in refluxing toluene yields $[\text{Al}_3(\text{tBu})_4\text{H}(\text{neol})_2]$ (**4**). The reflux conditions were necessary for reaction to occur. Compound **4** is also formed from the reaction of $\text{AlH}_2(\text{tBu})(\text{NMe}_3)$, see Experimental section.

Our initial attempts to characterize compound **4** crystallographically were hampered by the formation, as an impurity, of $[\text{Al}_3(\text{tBu})_4\text{Cl}(\text{neol})_2]$ (**5**). Compound **5** is presumably formed

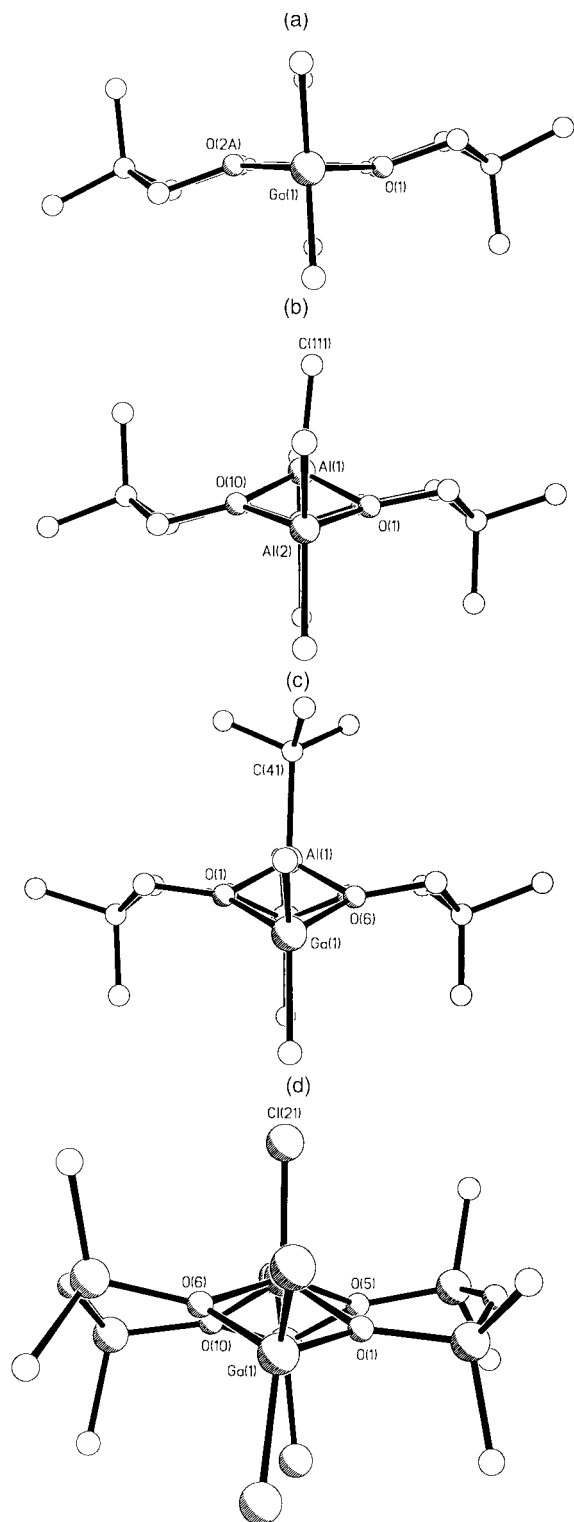


Fig. 3 Partial coordination sphere of (a) $[\text{Ga}_2(\text{'Bu})_4(\text{neol-H})_2]$ (**2**), (b) $[\text{Al}_3(\text{'Bu})_4\text{Me}(\text{neol})_2]$ (**6**) and (c) $[\text{Ga}_2\text{Al}(\text{'Bu})_4\text{Me}(\text{neol})_2]$ (**9**) viewed along the $\text{M} \cdots \text{M}$ vector showing the orientation of the neol CH_3 groups. The partial coordination sphere of (d) $[\text{Ga}_3\text{Cl}_5(\text{OSiMe}_2\text{-OSiMe}_2\text{O})_2]$ (**14**) is also shown for comparison.

owing to the presence of $\text{AlH}_2\text{Cl}(\text{NMe}_3)$ due to the excess of $[\text{Me}_3\text{NH}]\text{Cl}$ used in the synthesis of $\text{AlH}_3(\text{NMe}_3)$.¹¹ Reaction of compound **1** with AlMe_3 in refluxing toluene yields $[\text{Al}_3(\text{'Bu})_4\text{Me}(\text{neol})_2]$ (**6**), however, $[\text{Al}_3(\text{'Bu})_5(\text{neol})_2]$ could not be formed from the reaction with $\text{Al}(\text{'Bu})_3$ even when the reaction was carried out in refluxing toluene. In contrast, the reaction of $[\text{Ga}_2(\text{'Bu})_4(\text{neol-H})_2]$ (**2**) with $\text{Ga}(\text{'Bu})_3$ does result in the formation of $[\text{Ga}_3(\text{'Bu})_5(\text{neol})_2]$ (**7**). Compounds **4–7** have been spectroscopically and crystallographically characterized, see Experimental section and below.

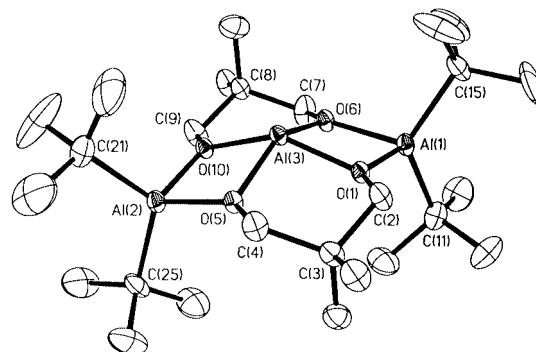
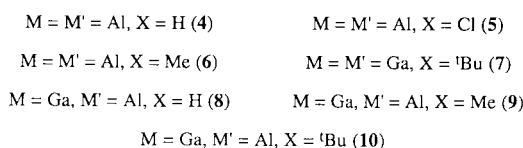
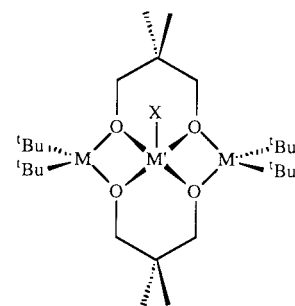


Fig. 4 Molecular structure of $[\text{Al}_3(\text{'Bu})_4\text{H}(\text{neol})_2]$ (**4**). Thermal ellipsoids are shown at the 30% level and all hydrogens are omitted for clarity.

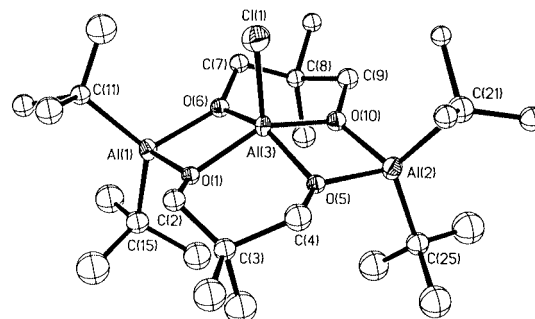


Fig. 5 Molecular structure of $[\text{Al}_3(\text{'Bu})_4\text{Cl}(\text{neol})_2]$ (**5**). Thermal ellipsoids are shown at the 30% level and all hydrogens are omitted for clarity.

The ease of synthesis of $[\text{Ga}_3(\text{'Bu})_5(\text{neol})_2]$ (**7**) and the inability to prepare $[\text{Ga}_2(\text{'Bu})_4(\text{neol-H})_2]$ (**2**) was more reactive than $[\text{Al}_2(\text{'Bu})_4(\text{neol-H})_2]$ and, thus, it was decided that compound **2** would make the better starting material for the heterometallic compounds, $[\text{M}_2\text{M}'(\text{'Bu})_4(\text{X})(\text{neol})_2]$. This rationale appeared to be correct since the reaction of compound **2** with $\text{AlH}_3(\text{NMe}_3)$ and AlMe_3 to yield $[\text{Ga}_2\text{Al}(\text{'Bu})_4\text{H}(\text{neol})_2]$ (**8**) and $[\text{Ga}_2\text{Al}(\text{'Bu})_4\text{Me}(\text{neol})_2]$ (**9**), respectively, occurs at room temperature in contrast to the high temperature synthesis of their tri-aluminium analogs. Similarly, whereas no reaction was observed between $\text{Al}(\text{'Bu})_3$ and compound **1**, the reaction with compound **2** occurs, albeit at high temperature (refluxing toluene solution), to give $[\text{Ga}_2\text{Al}(\text{'Bu})_5(\text{neol})_2]$ (**10**). Compounds **8–10** have been spectroscopically and crystallographically characterized, see Experimental section and below.

The molecular structures of compounds **4–10** are shown in Fig. 4–10 respectively; selected bond lengths and angles are given in Table 2. Each consists of a tetracycle structure formed

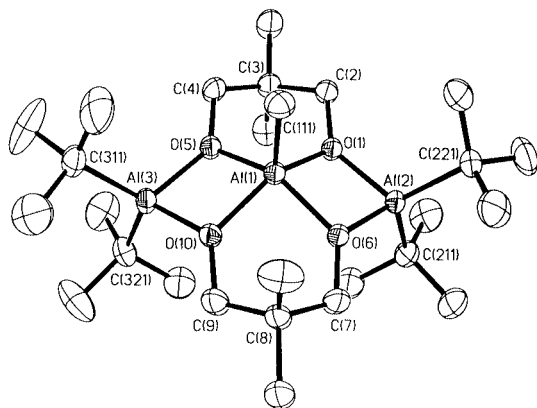


Fig. 6 Molecular structure of $[\text{Al}_3(\text{tBu})_4\text{Me}(\text{neol})_2]$ (**6**). Thermal ellipsoids are shown at the 30% level and all hydrogens are omitted for clarity.

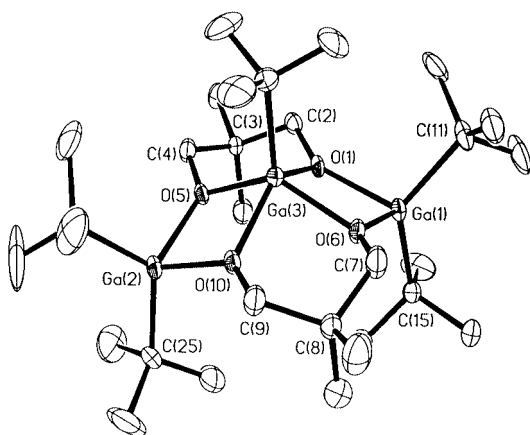


Fig. 7 Molecular structure of $[\text{Ga}_3(\text{tBu})_5(\text{neol})_2]$ (**7**). Thermal ellipsoids are shown at the 30% level and all hydrogens are omitted for clarity.

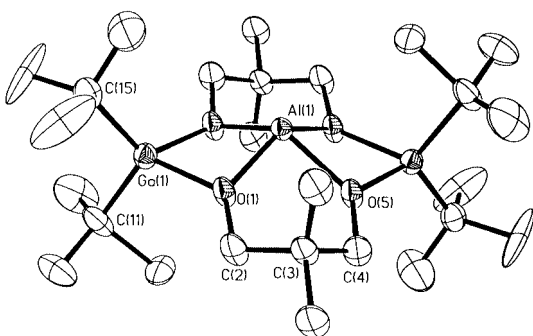


Fig. 8 Molecular structure of $[\text{Ga}_2\text{Al}(\text{tBu})_4\text{H}(\text{neol})_2]$ (**8**). Thermal ellipsoids are shown at the 30% level and all hydrogens are omitted for clarity.

from two 4-membered and two 6-membered rings. The bond lengths and angles are within the ranges expected. The central metal atom adopts a square based pyramidal structure, in which four oxygen atoms occupy the basal sites.

The central metal atoms in compounds **4–10** are displaced out from the O_4 plane. It may be expected that the magnitude of displacement would depend on either the steric bulk of the substituent on the central metal (*i.e.*, H *versus* Me *versus* tBu) or the identity of the central metal (*i.e.*, Al *versus* Ga). The steric bulk of the substituent on the central metal appears to make little difference in the displacement of the central metal atom out from the O_4 plane, suggesting that steric hindrance within the pocket is not an issue. In fact viewing a space filling diagram, it is clear that even with the *tert*-butyl substituent, there is little steric interaction between the substituent on the central metal

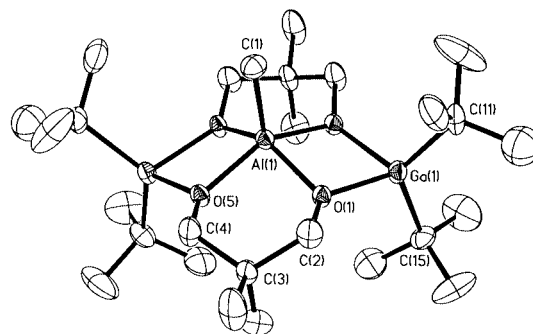


Fig. 9 Molecular structure of $[\text{Ga}_2\text{Al}(\text{tBu})_4\text{Me}(\text{neol})_2]$ (**9**). Thermal ellipsoids are shown at the 30% level and all hydrogens are omitted for clarity.

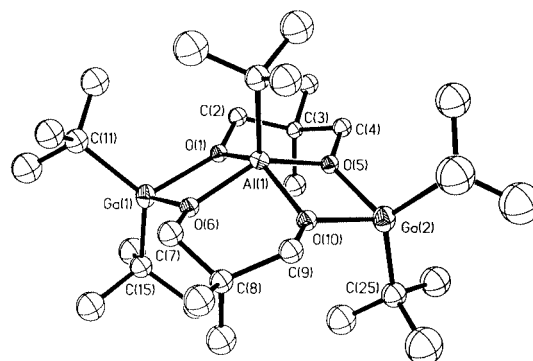


Fig. 10 Molecular structure of $[\text{Ga}_2\text{Al}(\text{tBu})_5(\text{neol})_2]$ (**10**). Thermal ellipsoids are shown at the 30% level and all hydrogens are omitted for clarity.

atom and the substituents on the neols. However, a comparison of the displacement of the central metal atom out from the O_4 plane in compounds **7** (0.78 Å) and **10** (0.66 Å) shows that Ga is further displaced than Al. This would be expected based on atom size. A comparison of compounds **6** (0.62 Å) and **9** (0.58 Å) suggests that $[\text{Ga}_2(\text{tBu})_4(\text{neol-H})_2]$ (**2**) has a bigger cavity than $[\text{Al}_2(\text{tBu})_4(\text{neol-H})_2]$ (**1**).

The distance between opposite oxygen atoms [*i.e.*, $\text{O}(1) \cdots \text{O}(10)$ or $\text{O}(1) \cdots \text{O}(1a)$ depending on the symmetry of the molecule] changes upon addition of a central metal atom. However, the direction of the changes are dependent on the identity of the central atom. Thus, the $\text{O} \cdots \text{O}$ distance increases with the inclusion of the same element, *i.e.*, 3.74 Å for $[\text{Ga}_3(\text{tBu})_5(\text{neol})_2]$ *versus* 3.62 Å for $[\text{Ga}_2(\text{tBu})_4(\text{neol-H})_2]$. However, inclusion of an aluminium into a gallium cycle results in a decrease in the $\text{O} \cdots \text{O}$ distance, *i.e.*, 3.52 Å for $[\text{Ga}_2\text{Al}(\text{tBu})_5(\text{neol})_2]$ *versus* 3.62 Å for $[\text{Ga}_2(\text{tBu})_4(\text{neol-H})_2]$. Thus, the cavity size appears to be moderately flexible and alters to accommodate the central metal.

As was observed for compounds **1** and **2**, the quaternary carbons of the neol rings in compounds **4–10** are displaced from the planar arrangement of the remaining atoms of the 6-membered M-O-C-C-C-O cycles, with the methyl groups adopting axial and equatorial positions. For compounds **4**, **5**, **6** and **8** one ring is in the chair conformation and the other in a boat conformation, *e.g.*, Fig. 3b. With increased steric bulk or decreased size of the central atom then both rings adopt a chair conformation, see Fig. 3c and d.

Unlike the parent compounds (**1–3**), ^1H and ^{13}C NMR spectra of compounds **4–10** (see Experimental section) show a different magnetic environment for the tBu protons. The CH_2 of the neol ligand are also inequivalent and appear as AB quartets in the ^1H NMR spectrum. This is diagnostic of the trimeric structural motif. The CH_3 carbons become inequivalent but the CH_2 carbons remain equivalent in ^{13}C NMR spectrum. For $[\text{Al}_3(\text{tBu})_4(\text{Me})(\text{neol})_2]$ (**6**) and $[\text{Ga}_2\text{Al}(\text{tBu})_4(\text{Me})(\text{neol})_2]$ (**9**) only

Table 2 Selected bond lengths (Å) and angles (°) in [M₂M'('Bu)₄(X)(neol)₂]

Compound	M	M'	X	M–O	M'–O	M'–X	C–M–C	O–M–O	O–M'–O _{cis} ^d	O–M'–O _{trans} ^d
4a	Al	Al	H	1.815(5)	1.877(5)	^b	122.0(3)	78.7(2)	77.8(2)	144.5(2)
				1.821(5)	1.871(5)		119.3(3)	80.6(2)	78.2(2)	144.6(3)
				1.860(5)	1.868(6)				90.6(2)	
				1.862(6)	1.868(5)				92.0(2)	
5	Al	Al	Cl	1.82(3)	1.82(3)	2.12(8) ^c	120(2)	76(1)	76(1)	146.4(6)
				1.84(2)	1.83(3)		121(2)	80(1)	80(1)	147.9(6)
				1.85(3)	1.85(3)				92(1)	
				1.89(3)	1.87(3)				93(1)	
6	Al	Al	Me	1.825(2)	1.873(2)	1.963(3)	118.7(1)	79.35(9)	77.16(9)	140.91(9)
				1.832(2)	1.876(2)		119.1(1)	79.49(9)	77.36(9)	142.13(9)
				1.845(2)	1.884(2)				89.91(9)	
				1.846(2)	1.887(2)				90.83(9)	
7^a	Ga	Ga	'Bu	1.878(4)	1.898(4)	2.041(7)	124.6(3)	88.4(2)	73.6(2)	132.6(2)
				1.936(4)	1.972(4)		124.9(3)	88.8(2)	76.5(2)	134.8(2)
				1.981(4)	2.016(4)				86.5(2)	
				2.023(4)	2.041(4)				87.7(2)	
8^a	Ga	Al	H	1.927(4)	1.858(5)	^b	114.0(7)	75.8(2)	73.3(2)	133.2(2)
				1.934(4)	1.971(5)				78.3(2)	133.3(2)
									85.1(2)	
									87.0(2)	
9	Ga	Al	Me	1.955(4)	1.867(4)	1.96(1)	124.8(4)	74.4(2)	78.4(2)	143.4(3)
				1.951(4)	1.869(4)				90.6(2)	144.6(3)
10^a	Ga	Al	'Bu	1.948(4)	1.874(4)	2.023(7)	119.7(3)	73.6(2)	77.0(2)	139.2(2)
				1.952(4)	1.885(4)		120.8(4)	74.4(2)	77.2(2)	139.4(2)
				1.952(4)	1.888(4)				88.5(2)	
				1.958(4)	1.893(4)				89.3(2)	

^a Where crystallographic disorder is present distances from only one molecule are included. ^b Not located, see Experimental section. ^c Partial occupancy; disorder between Cl and H, see text. ^d Geometry is near square based pyramid. *cis* and *trans* is with relationship to basal oxygen atoms.

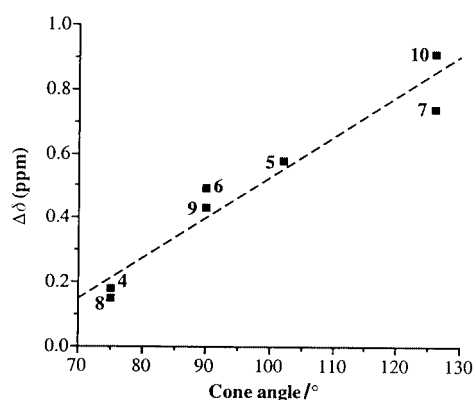


Fig. 11 Plot of chemical shift difference ($\Delta\delta$, ppm) as a function of the Tolman cone angle (θ°) for the central metal atom substituents (X) in [M₂M'('Bu)₄(X)(neol)₂]. See text for compound numbers.

one type of C(CH₃)₃ is observed in the ¹H NMR spectrum but 2 C(CH₃)₃ are observed in the ¹³C NMR spectrum. This implies that there is accidental overlap of two signals in the ¹H NMR spectrum. This is confirmed by examination of the ¹H NMR spectrum of **6** in C₇D₈ at 70 °C in which two *tert*-butyl peaks are seen at δ 1.18 and 1.16. The chemical shifts of the inequivalent equatorial and axial methyl groups in each trimetallic species vary greatly. In most cases the axial and equatorial methyl groups are shifted similarly in opposite directions from those of the dimers [Al₂('Bu)₄(neol-H)₂] (**1**) ($\Delta\delta$ = 0.65 ppm) and [Ga₂('Bu)₄(neol-H)₂] (**2**) ($\Delta\delta$ = 0.78 ppm). The size of the shift seems to depend on the size of the substituent on the central metal atom, the larger the central group the bigger the chemical shift (see Fig. 11). The ¹³C NMR chemical shift is not as sensitive to this effect as the ¹H NMR spectrum. NOE experiments indicate that the peaks to downfield are those *syn* to the substituent on the central metal atom.

As noted in the Introduction, Ziemkowska and Pasynkiewicz⁴ have previously reported the synthesis of [Al₃Me₃(neol)₂], as well as several compounds derived from similar substituted 1,3-diols. These researchers did not isolate any intermediates

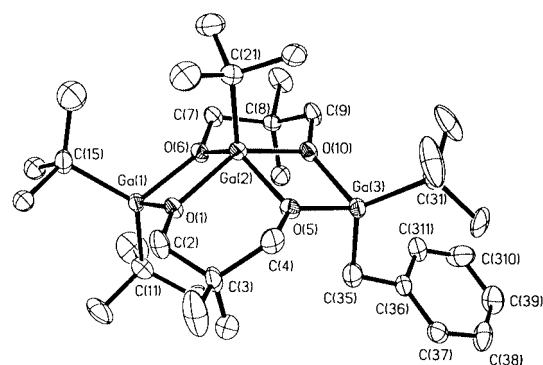


Fig. 12 The molecular structure of [Ga₃('Bu)₄(CH₂Ph)(neol)₂] (**11**). Thermal ellipsoids are shown at the 30% level, and all hydrogens are omitted for clarity.

analogous to compound **1**, and instead proposed a reaction involving the formation of [AlR(neol)] and [(AlR)₂(neol)]. Given our isolation of compound **1**, and its subsequent conversion to the tri-aluminium compounds, we propose that the methyl analog of compound **1** is undoubtedly formed as an intermediate in the formation of [Al₃Me₃(neol)₂] from AlMe₃ and neol-H₂.

Decomposition of [Ga₂('Bu)₄(neol-H)₂]

An unusual decomposition product was observed during the thermolysis of a batch of [Ga₂('Bu)₄(neol-H)₂] in toluene, [Ga₂('Bu)₄(CH₂Ph)(neol)₂] (**11**), see Experimental section. The molecular structure of compound **11** is shown in Fig. 12; selected bond lengths and angles are given in Table 3. The molecular structure of compound **11** is similar to that of [Ga₃('Bu)₅(neol)₂] (**7**), but one of the *tert*-butyl ligands on the exocyclic gallium centers has been replaced with a benzyl group. We are unsure what catalyzed the loss of butane in this reaction which is possibly radical in nature. It should be noted that compound **11** is not formed from [Ga₃('Bu)₅(neol)₂] (**7**) under similar conditions. Benzyl derivatives of gallium are well known and several have been structurally characterized.¹²

Table 3 Bond lengths (Å) and angles (°) in $[\text{Ga}_3(\text{tBu})_4(\text{CH}_2\text{Ph})(\text{neol})_2]$ (**11**)

Ga(1)–O(1)	1.919(9)	Ga(1)–O(6)	1.956(8)
Ga(1)–C(15)	2.00(2)	Ga(1)–C(11)	2.02(2)
Ga(2)–O(6)	1.933(9)	Ga(2)–O(5)	1.968(9)
Ga(2)–O(1)	1.975(8)	Ga(2)–C(21)	1.98(2)
Ga(2)–O(10)	1.993(8)	Ga(3)–O(10)	1.931(9)
Ga(3)–O(5)	1.931(8)	Ga(3)–C(35)	1.94(2)
Ga(3)–C(31)	2.01(1)		
O(1)–Ga(1)–O(6)	74.5(4)	O(1)–Ga(1)–C(15)	109.7(6)
O(6)–Ga(1)–C(15)	113.0(5)	O(1)–Ga(1)–C(11)	115.6(5)
O(6)–Ga(1)–C(11)	114.3(5)	C(15)–Ga(1)–C(11)	120.7(7)
O(6)–Ga(2)–O(5)	132.9(4)	O(6)–Ga(2)–O(1)	73.8(3)
O(5)–Ga(2)–O(1)	88.2(4)	O(6)–Ga(2)–C(21)	116.1(6)
O(5)–Ga(2)–C(21)	110.9(6)	O(1)–Ga(2)–C(21)	116.9(5)
O(6)–Ga(2)–O(10)	86.6(4)	O(5)–Ga(2)–O(10)	74.5(3)
O(1)–Ga(2)–O(10)	133.1(4)	C(21)–Ga(2)–O(10)	110.0(5)
O(10)–Ga(3)–O(5)	76.8(4)	O(10)–Ga(3)–C(35)	108.4(6)
O(5)–Ga(3)–C(35)	107.4(5)	O(10)–Ga(3)–C(31)	116.0(5)
O(5)–Ga(3)–C(31)	115.7(5)	C(35)–Ga(3)–C(31)	123.1(7)
Ga(1)–O(1)–Ga(2)	105.6(4)	C(4)–O(5)–Ga(3)	134.4(9)
Ga(3)–O(5)–Ga(2)	104.8(4)	Ga(2)–O(6)–Ga(1)	105.8(4)
Ga(3)–O(10)–Ga(2)	103.9(4)		

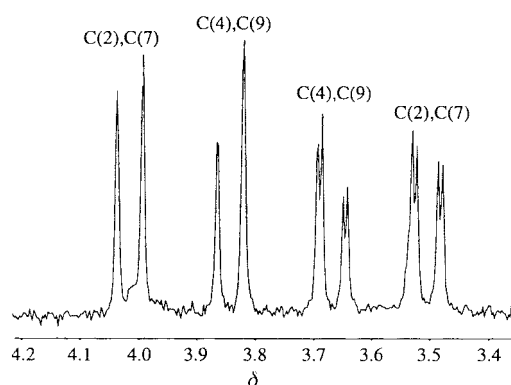


Fig. 13 The ^1H NMR spectrum of the neol's CH_2 groups in $[\text{Ga}_2(\text{tBu})_4(\text{CH}_2\text{Ph})(\text{neol})_2]$ (**11**), showing the AA'BB' pattern and presence of 4-bond coupling [$J(\text{H}-\text{H}) \approx 2$ Hz] between axial-CH protons on carbon atoms of the same ligand. For assignment of peaks see atom numbering scheme in Fig. 12.

Due to the replacement of one *tert*-butyl ligand with benzyl ligand the C_2 symmetry in $[\text{Ga}_3(\text{tBu})_5(\text{neol})_2]$ (**7**) is lost, resulting in a complicated AA'BB' pattern in the ^1H NMR spectrum of the neol's CH_2 region, see Fig. 13. What is interesting to note is the presence of an unusual 4-bond coupling [$J(\text{H}-\text{H}) \approx 2$ Hz] between the axial CH protons on carbon atoms of the same ligand. This is presumably allowed due to a rigid conformation of the neol $\text{CH}_2\text{-CMe}_2\text{-CH}_2$ backbone.

Reaction of $[\text{Ga}(\text{tBu})_2(\text{neol-H})_2]$ with CaH_2 and LiOH

A low yield conversion of $[\text{Ga}_2(\text{tBu})_4(\text{neol-H})_2]$ (**2**) to $[\text{Ga}_3(\text{tBu})_5(\text{neol})_2]$ (**7**) occurs upon heating in toluene in the presence of CaH_2 (ca. 50% yield). A similar rearrangement occurs in the presence of Mg (ca. 50% yield). In neither case have we been able to identify the other products from these reactions.

Heating compound **2** in the presence of LiOH (in Et_2O) results, after recrystallization from THF, in the isolation of the trimeric species $[\text{Ga}_3\text{Li}_4(\text{tBu})_6(\text{neol})_3(\text{OH})(\text{THF})]$ (**12**). It is interesting to note that a formal rearrangement to a trimer has occurred. The molecular structure of $[\text{Ga}_3\text{Li}_4(\text{tBu})_6(\text{neol})_3(\text{OH})(\text{THF})]$ (**12**) has been determined by X-ray crystallography and is shown in Fig. 14. Due to the high e.s.d.s only a discussion of the overall structure may be made. The structure of compound **12** consists of a $\text{Ga}_3\text{O}_6\text{C}_9$ macrocycle encompassing four lithium atoms in turn capped by a hydroxide. The core of this $\text{Ga}_3\text{Li}_4\text{O}_6$ cluster consists of seven fused 4-membered rings

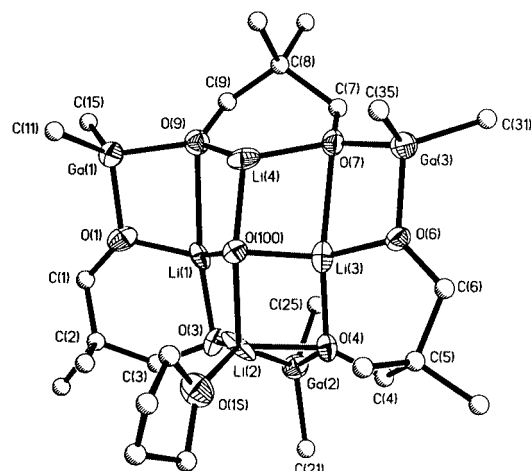


Fig. 14 The molecular structure of $[\text{Ga}_3\text{Li}_4(\text{tBu})_6(\text{neol})_3(\text{OH})(\text{THF})]$ (**12**). Thermal ellipsoids are shown at the 20% level. Carbon atoms are shown as shaded spheres and *tert*-butyl methyl groups are omitted for clarity. Selected bond lengths: Ga(1)–O(1) = 1.86(1), Ga(1)–O(9) = 1.92(2), Ga(2)–O(4) = 1.92(1), Ga(2)–O(3) = 1.95(1), Ga(3)–O(7) = 1.88(1), Ga(3)–O(6) = 1.89(1), Li(1)–O(1) = 1.82(4), Li(1)–O(3) = 1.91(4), Li(2)–O(3) = 1.96(5), Li(2)–O(4) = 1.99(4), Li(2)–O(15) = 2.00(4), Li(3)–O(4) = 1.97(4), Li(3)–O(6) = 1.80(4), Li(4)–O(7) = 1.92(5), Li(4)–O(9) = 1.79(4) Å.

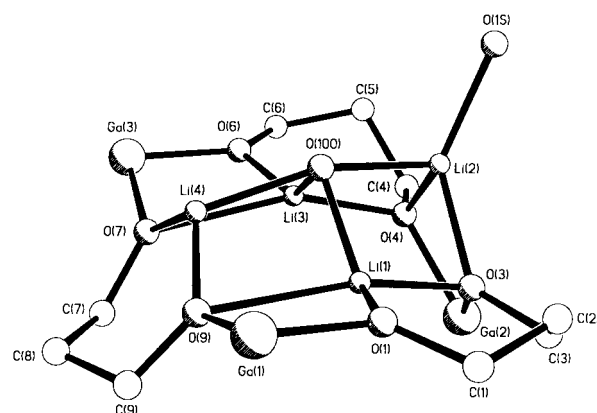


Fig. 15 The structure of core of $[\text{Ga}_3\text{Li}_4(\text{tBu})_6(\text{neol})_3(\text{OH})(\text{THF})]$ (**12**). The *tert*-butyl groups and carbon atoms of the THF ligand are omitted for clarity.

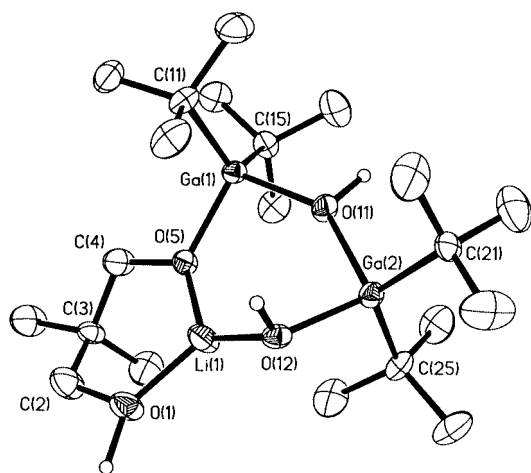
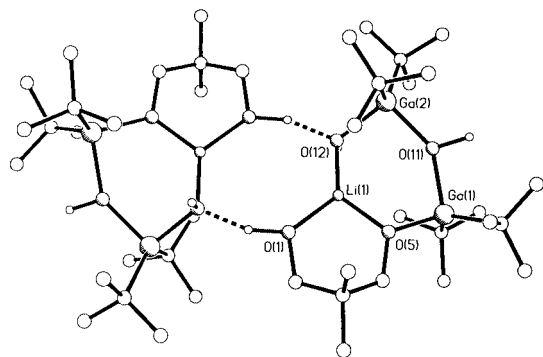
an unusual geometry (Fig. 15). Compound **12** may be described as a Schiff base-like cryptane analogous to 18-crown-6. The size of the cavity should be sufficient to complex a variety of transition metal and main group metals.

The reaction of compound **2** with LiOH in hexane results in the isolation of $[\text{Ga}_2\text{Li}(\text{tBu})_4(\text{OH})_2(\text{neol-H})]$ (**13**). The IR spectrum shows a sharp OH stretch at 3625 cm^{-1} . The molecular structure of **13** is shown in Fig. 16 and selected bond angles and lengths are given in Table 4. The core of compound **13** consists of a Ga_2LiO_3 cycle, in which Li(1) is chelated by the neol-H ligand. All bond lengths and angles are within the ranges expected.¹³ The hydroxide hydrogen atoms were located and while O(11) adopts a planar geometry as has been observed for other aluminium and gallium bridging hydroxides,¹⁴ O(12) appears to be tetrahedral. The reason for the non-planar geometry is readily seen from a consideration of the extended structure, see Fig. 17. Compound **13** forms hydrogen bonded dimers in the solid state. The $\text{O}\cdots\text{O}$ distance (2.72 Å) is typical for such interactions.¹⁵ No hydrogen bonding is observed to O(11), presumably due to the steric bulk of the adjacent $\text{Ga}(\text{tBu})_2$ moieties.

It is interesting to note that no loss of gallium alkyls has occurred in the formation of compound **13**. Instead, compound **13** may best be considered to be the result of ligand substitution

Table 4 Bond lengths (Å) and angles (°) in $[\text{Ga}_2\text{Li}(\text{tBu})_4(\text{OH})_2(\text{neol-H})]$ (**13**)

Ga(1)–O(5)	1.884(4)	Ga(1)–O(11)	1.974(4)
Ga(1)–C(11)	2.000(7)	Ga(1)–C(15)	2.004(7)
Ga(2)–O(12)	1.919(4)	Ga(2)–O(11)	1.958(4)
Ga(2)–C(21)	2.001(7)	Ga(2)–C(25)	1.998(7)
O(1)–C(2)	1.445(9)	O(1)–Li(1)	1.85(1)
O(5)–C(4)	1.424(8)	O(5)–Li(1)	1.82(1)
O(12)–Li(1)	1.90(1)		
O(5)–Ga(1)–O(11)	96.3(2)	O(5)–Ga(1)–C(11)	109.4(3)
O(11)–Ga(1)–C(11)	105.7(2)	O(5)–Ga(1)–C(15)	112.7(2)
O(11)–Ga(1)–C(15)	104.9(3)	C(11)–Ga(1)–C(15)	123.8(3)
O(12)–Ga(2)–O(11)	96.3(2)	O(12)–Ga(2)–C(21)	113.3(3)
O(11)–Ga(2)–C(21)	105.0(2)	O(12)–Ga(2)–C(25)	106.1(3)
O(11)–Ga(2)–C(25)	107.1(2)	C(21)–Ga(2)–C(25)	125.0(3)
C(4)–O(5)–Ga(1)	116.1(4)	Li(1)–O(5)–Ga(1)	121.5(4)
Ga(2)–O(11)–Ga(1)	144.3(2)	Li(1)–O(12)–Ga(2)	109.6(5)
O(5)–Li(1)–O(1)	104.6(7)	O(5)–Li(1)–O(12)	125.7(7)
O(1)–Li(1)–O(12)	128.7(7)		

**Fig. 16** The molecular structure of $[\text{Ga}_2\text{Li}(\text{tBu})_4(\text{OH})_2(\text{neol-H})]$ (**13**). Thermal ellipsoids are shown at the 30% level, and all hydrogens are omitted for clarity.**Fig. 17** The hydrogen bonded structure of $[\text{Ga}_2\text{Li}(\text{tBu})_4(\text{OH})_2(\text{neol-H})]$ (**13**).

(neol-H for OH), and complexation with one equivalent of LiOH.

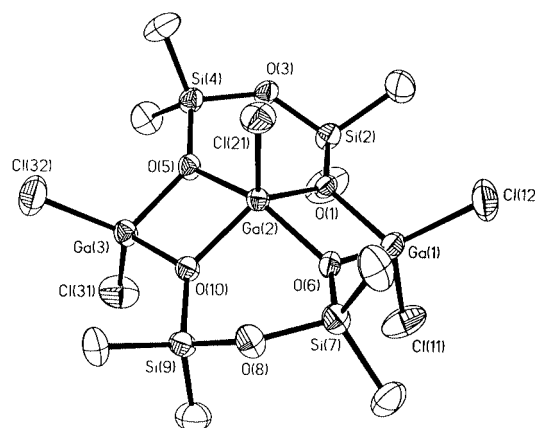
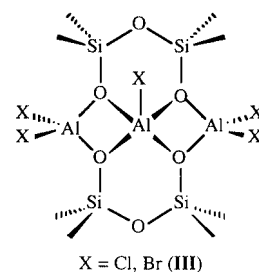
Trimetallic siloxane $[\text{M}_3\text{Cl}_5(\text{OSiMe}_2\text{OSiMe}_2\text{O})_2]$

The aluminosiloxanes, $[\text{M}_3\text{X}_5(\text{OSiMe}_2\text{OSiMe}_2\text{O})_2]$, (**III**, X = Cl,¹⁶ Br,¹⁷) are isostructural to the tri-metallic compounds, $[\text{M}_2\text{M}'(\text{tBu})_4(\text{X})(\text{neol})_2]$, described above.

Both aluminosiloxanes have been previously characterized by X-ray crystallography, however, no spectroscopic characterization was reported. We have prepared the chloride derivative and report its spectroscopic characterization, see Experimental section. In addition, we have prepared and structurally charac-

Table 5 Bond lengths (Å) and angles (°) in $[\text{Ga}_3\text{Cl}_5(\text{OSiMe}_2\text{OSiMe}_2\text{O})_2]$ (**14**)

Ga(1)–O(6)	1.859(5)	Ga(1)–O(1)	1.889(5)
Ga(1)–Cl(12)	2.121(3)	Ga(1)–Cl(11)	2.125(3)
Ga(2)–O(10)	1.934(5)	Ga(2)–O(1)	1.943(5)
Ga(2)–O(6)	1.958(5)	Ga(2)–O(5)	1.989(5)
Ga(2)–Cl(21)	2.139(2)	Ga(3)–O(5)	1.869(5)
Ga(3)–O(10)	1.895(5)	Ga(3)–Cl(32)	2.117(3)
Ga(3)–Cl(31)	2.119(3)	Si(2)–O(3)	1.608(6)
Si(2)–O(1)	1.688(5)	Si(4)–O(3)	1.644(6)
Si(4)–O(5)	1.677(5)	Si(7)–O(8)	1.626(6)
Si(7)–O(6)	1.701(5)	Si(9)–O(8)	1.632(6)
Si(9)–O(10)	1.696(5)		
O(6)–Ga(1)–O(1)	82.0(2)	O(6)–Ga(1)–Cl(12)	113.4(2)
O(1)–Ga(1)–Cl(12)	116.0(2)	O(6)–Ga(1)–Cl(11)	114.6(2)
O(1)–Ga(1)–Cl(11)	112.1(2)	Cl(12)–Ga(1)–Cl(11)	114.7(2)
O(10)–Ga(2)–O(1)	133.5(2)	O(10)–Ga(2)–O(6)	91.2(2)
O(1)–Ga(2)–O(6)	78.2(2)	O(10)–Ga(2)–O(5)	79.1(2)
O(1)–Ga(2)–O(5)	91.5(2)	O(6)–Ga(2)–O(5)	154.6(2)
O(10)–Ga(2)–Cl(21)	112.9(2)	O(1)–Ga(2)–Cl(21)	113.6(2)
O(6)–Ga(2)–Cl(21)	103.0(2)	O(5)–Ga(2)–Cl(21)	102.4(2)
O(5)–Ga(3)–O(10)	83.2(2)	O(5)–Ga(3)–Cl(32)	112.5(2)
O(10)–Ga(3)–Cl(32)	114.8(2)	O(5)–Ga(3)–Cl(31)	113.4(2)
O(10)–Ga(3)–Cl(31)	112.0(2)	Cl(32)–Ga(3)–Cl(31)	116.5(1)
O(3)–Si(2)–O(1)	106.1(3)	O(3)–Si(4)–O(5)	103.0(3)
O(8)–Si(7)–O(6)	102.5(3)	O(8)–Si(9)–O(10)	105.5(3)
Si(2)–O(1)–Ga(1)	128.7(3)	Si(2)–O(1)–Ga(2)	131.4(3)
Ga(1)–O(1)–Ga(2)	99.6(2)	Si(2)–O(3)–Si(4)	137.5(4)
Si(4)–O(5)–Ga(3)	132.7(3)	Si(4)–O(5)–Ga(2)	128.8(3)
Ga(3)–O(5)–Ga(2)	98.3(2)	Si(7)–O(6)–Ga(1)	130.5(3)
Si(7)–O(6)–Ga(2)	128.8(3)	Ga(1)–O(6)–Ga(2)	100.1(2)
Si(7)–O(8)–Si(9)	134.1(4)	Si(9)–O(10)–Ga(3)	129.8(3)
Si(9)–O(10)–Ga(2)	130.8(3)	Ga(3)–O(10)–Ga(2)	99.4(2)

**Fig. 18** The molecular structure of $[\text{Ga}_3\text{Cl}_5(\text{OSiMe}_2\text{OSiMe}_2\text{O})_2]$ (**14**). Thermal ellipsoids are shown at the 30% level, and all hydrogens are omitted for clarity.

terized the gallium siloxane, $[\text{Ga}_3\text{Cl}_5(\text{OSiMe}_2\text{OSiMe}_2\text{O})_2]$ (**14**) as a minor product in the reaction of GaCl_3 with $(\text{OSiMe}_2)_4$, see Experimental section.

The molecular structure of $[\text{Ga}_3\text{Cl}_5(\text{OSiMe}_2\text{OSiMe}_2\text{O})_2]$ (**14**) is shown in Fig. 18; selected bond lengths and angles are given in Table 5. All the bond lengths and angles are within the ranges expected.^{18,19} It is interesting to compare the structures of $[\text{Al}_3\text{Cl}_5(\text{OSiMe}_2\text{OSiMe}_2\text{O})_2]$ and compound **14** with $[\text{Al}_3-$

(^tBu)₄Cl(neol)₂] (**5**). Whereas the AlO₂C₃ cycles in compound **5** adopt a chair conformation in order to limit steric interactions between the neol's methyl groups and the aluminium chloride, the AlO₃Si₂ cycles in [Al₃Cl₅(OSiMe₂OSiMe₂O)₂]¹⁷ and compound **14** adopt boat conformations (Fig. 3d).

Experimental section

All operations were carried out under inert atmosphere using Schlenk techniques or VAC inert atmosphere dry box. Mass spectra were obtained on a Finnigan MAT 95 mass spectrometer operating with an electron beam energy of 70 eV for EI mass spectra. IR spectra (4000–400 cm^{−1}) were obtained using a Nicolet 760 FT-IR infrared spectrometer. Samples were prepared as Nujol mulls between KBr plates unless otherwise stated. NMR spectra were obtained on Bruker AM-250 and Avance 200 spectrometers. Chemical shifts are reported relative to internal solvent resonances (¹H and ¹³C), and external [Al(H₂O)₆]³⁺ (²⁷Al). Microanalyses were performed by Oneida Research Services, Inc., Whitesboro, NY, USA. The syntheses of Al(^tBu)₃, Ga(^tBu)₃ and ^tBuAlH₂(NMe₃) and were performed according to the literature methods.^{20,21} neol-H₂ (HOCH₂CMe₂CH₂OH) was generously donated by BASF.

Syntheses

[Al₂(^tBu)₄(neol-H)₂] (**1**). neol-H₂ (0.25 g, 2.4 mmol) was suspended in hexane (150 cm³) and cooled to −78 °C. To this was added a solution of Al(^tBu)₃ (0.5 g, 2.4 mmol) in hexane (30 cm³). After addition, the reaction was allowed to warm to room temperature. The solution was stirred for 1 day, filtered and placed in freezer. X-Ray quality crystals were formed overnight. Yield: 0.46 g, 78%; mp 163 °C. Analysis (calc., %): Al, 11.1 (11.0). MS (EI, %): *m/z* 431 (M⁺ − ^tBu, 100), 373 (M⁺ − 2 ^tBu, 92), 315 (M⁺ − 3 ^tBu, 23), 187 [(^tBu)Al(neol-H), 23], 57 (^tBu, 53). IR (cm^{−1}): 2694 (m), 1670 (w, br), 1257 (m), 1062, 1020 (br), 805 (s), 600 (s). ¹H NMR (C₆D₆): δ 16.16 (2H, s, OH), 3.72 (8H, s, CH₂), 1.23 [36H, s, C(CH₃)₃], 0.65 [12H, s, C(CH₃)₂]. ¹³C NMR (C₆D₆): δ 77.2 (CH₂), 33.4 [C(CH₃)₂], 31.1 [C(CH₃)₃], 22.1 (CH₃).

[Ga₂(^tBu)₄(neol-H)₂] (**2**). Prepared in the same manner to compound **1**, but using neol-H₂ (1.0 g, 9.6 mmol) and Ga(^tBu)₃ (2.8 g, 11.6 mmol). Yield: 2.0 g, 72%; mp 192–195 °C. Analysis (calc., %): C, 54.61 (54.38); H, 10.01 (9.83). MS (EI, %): *m/z* 517 (M⁺ − ^tBu, 20), 183 [Ga(^tBu)₂, 60], 229 [(^tBu)Ga(neol-H), 25], 57 (^tBu, 60). IR (cm^{−1}): 1152 (w), 1055 (m), 1014 (m), 819 (s). ¹H NMR (C₆D₆): δ 15.01 (2H, s, OH), 3.74 (8H, s, OCH₂), 1.28 [36H, s, C(CH₃)₃], 0.78 [12H, s, C(CH₃)₂]. ¹³C NMR (CDCl₃): δ 78.1 (OCH₂), 34.7 [C(CH₃)₂], 30.4 [C(CH₃)₃], 22.6 [C(CH₃)₂].

[AlGa(^tBu)₄(neol-H)₂] (**3**). A pentane solution (100 cm³) containing Al(^tBu)₃ (1.0 g, 5.0 mmol) and Ga(^tBu)₃ (1.2 g, 5.0 mmol) was added at room temperature to a pentane solution (60 cm³) containing neol-H₂ (0.51 g, 5.0 mmol). The reaction was stirred for 18 hours, filtered and the hexane removed *in vacuo*. Based upon the ¹H NMR spectrum the crude reaction product was a mixture of compound **1** (18.7%), **2** (2.6%), [AlGa(^tBu)₄(neol-H)₂] (3.7%), [Ga₂Al(^tBu)₅(neol)₂] (compound **10**, see below) (22.5%) and unreacted Al(^tBu)₃ and Ga(^tBu)₃ (52.4%). The crude material was redissolved in hexane and the first precipitate consisted of compound **1** and [AlGa(^tBu)₄(neol-H)₂]. Repeated recrystallisations from hexane did not allow for full separation of compound **1** from [AlGa(^tBu)₄(neol-H)₂] (**3**). MS (EI, %): *m/z* 473 (M⁺ − ^tBu, 90), 416 (M⁺ − 2 ^tBu, 25), 187 [Ga(^tBu)₂, 40]. IR (cm^{−1}): 3751 (m, ν_{OH}), 2692 (m), 1398 (m), 1230 (s). ¹H NMR (C₆D₆): δ 15.41 (2H, s, OH), 3.83 (4H, s, CH₂), 3.63 (4H, s, CH₂), 1.32 [18H, s, C(CH₃)₃], 1.18 [18H, s, C(CH₃)₃], 0.72 [12H, s, C(CH₃)₂]. ¹³C NMR (C₆D₆): δ 76.8 (OCH₂), 76.5 (OCH₂), 32.4 [C(CH₃)₂], 30.5 [C(CH₃)₃], 31.4 [C(CH₃)₃], 25.2 [C(CH₃)₂].

[Al₃(^tBu)₄H(neol)₂] (**4**). *Method 1*. A mixture of [Al₂(^tBu)₄(neol-H)₂] (0.22 g, 0.45 mmol) and AlH₃(NMe₃) (0.08 g, 0.9 mmol) was refluxed in toluene overnight. The toluene was removed *in vacuo* and the resulting white powder was recrystallised from hexane at −23 °C. Yield: 0.14 g, 62%.

Method 2. A mixture of [Al₂(^tBu)₄(neol-H)₂] (0.3 g, 0.6 mmol) and AlH₂(^tBu)(NMe₃) (0.18 g, 1.2 mmol) was refluxed in toluene overnight. Removal of all volatiles under vacuum followed by recrystallisation from hexane gave white crystals. Yield: ca. 50%; mp >235 °C. MS (EI, %): *m/z* 457 (M⁺ − ^tBu, 100), 401 (M⁺ − 2 ^tBu, 22). IR (cm^{−1}): 1844 (m, ν_{AlH}), 1260 (w), 1061 (s), 1018 (s), 811 (m), 654 (s). ¹H NMR (C₆D₆): δ 3.68 [4H, d, *J*(H–H) = 10.3 Hz, CH₂], 3.47 [4H, d, *J*(H–H) = 10.3 Hz, CH₂], 1.28 [18H, s, C(CH₃)₃], 1.22 [18H, s, C(CH₃)₃], 0.74 [6H, s, C(CH₃)₂], 0.57 [6H, s, C(CH₃)₂]. ¹³C NMR (C₆D₆): δ 74.9 (OCH₂), 35.8 [C(CH₃)₂], 31.4 [C(CH₃)₃], 30.7 [C(CH₃)₃], 23.1 [C(CH₃)₂], 22.1 [C(CH₃)₂]. ²⁷Al NMR (C₆D₆/C₇H₈): δ 61 (W_{1/2} = 820 Hz).

[Al₃(^tBu)₄Cl(neol)₂] (**5**). Prepared in a similar manner to compound **4** except a mixture of AlH₂Cl(NMe₃) and AlH₃(NMe₃) was used. Yield ca. 30%. ¹H NMR (C₆D₆): δ 3.93 [4H, d, *J*(H–H) = 10.4 Hz, CH₂], 3.38 [4H, d, *J*(H–H) = 10.4 Hz, CH₂], 1.32 [18H, s, C(CH₃)₃], 1.20 [18H, s, C(CH₃)₃], 0.93 [6H, s, C(CH₃)₂], 0.35 [6H, s, C(CH₃)₂]. ¹³C NMR (C₆D₆): δ 75.3 (OCH₂), 35.6 [C(CH₃)₂], 31.8 [C(CH₃)₃], 30.8 [C(CH₃)₃], 23.9 [C(CH₃)₂], 21.5 [C(CH₃)₂].

[Al₃(^tBu)₄Me(neol)₂] (**6**). A mixture of [Al₂(^tBu)₄(neol-H)₂] (0.4 g, 0.82 mmol) and AlMe₃ (0.12 g, 1.7 mmol) was refluxed in toluene overnight. The toluene was removed *in vacuo* and the resulting white powder was recrystallised from hexane at −23 °C. Yield: 0.31 g, 72%, mp >235 °C. Analysis (calc., %): C, 61.05 (61.30); H, 11.20 (11.24). MS (EI, %): *m/z* 472 (M⁺ − ^tBu, 25), 415 (M⁺ − 2 ^tBu, 90), 317 (M⁺ − 3 ^tBu − AlMe, 42). IR (cm^{−1}): 2694 (m), 1406 (w), 1211 (m), 1070 (s), 1019 (s), 812 (s). ¹H NMR (C₆D₆): δ 3.67 [4H, d, *J*(H–H) = 10.8 Hz, CH₂], 3.44 [4H, d, *J*(H–H) = 10.8 Hz, CH₂], 1.24 [36H, s, C(CH₃)₃], 0.90 [6H, s, C(CH₃)₂], 0.41 [6H, s, C(CH₃)₂], −0.36 (3H, s, AlCH₃). ¹³C NMR (C₆D₆): δ 74.9 (CH₂), 35.7 [C(CH₃)₂], 31.9 [C(CH₃)₃], 31.1 [C(CH₃)₃], 24.0 [C(CH₃)₂], 21.9 [C(CH₃)₂], −13.7 (AlCH₃).

[Ga₃(^tBu)₅(neol)₂] (**7**). To a toluene (30 cm³) solution of [Ga₂(^tBu)₄(neol-H)₂] (1.0 g, 17.4 mmol) was added neat Ga(^tBu)₃ (4.2 g, 17.4 mmol). The reaction was refluxed overnight and the solvent then removed *in vacuo*. The resultant solid was recrystallised from hexane at −23 °C. Yield: 77%; mp 235–238 °C. MS (EI, %): *m/z* 641 (M⁺ − ^tBu, 50), 527 (M⁺ − 3 ^tBu, 20), 299 [Ga₂(^tBu)(neol), 20], 183 (Ga^tBu₂, 24), 57 (^tBu, 100). IR (cm^{−1}): 1576 (m), 1360 (s), 1059 (s), 1010 (s). ¹H NMR (C₆D₆): δ 3.98 [4H, d, *J*(H–H) = 11.0 Hz, CH₂], 3.56 [4H, d, *J*(H–H) = 11.0 Hz, CH₂], 1.47 [9H, s, C(CH₃)₃], 1.37 [18H, s, C(CH₃)₃], 1.35 [18H, s, C(CH₃)₃], 1.20 [6H, s, C(CH₃)₂], 0.46 [6H, s, C(CH₃)₂]. ¹³C NMR (C₆D₆): δ 78.4 (OCH₂), 37.6 [C(CH₃)₂], 34.0 [C(CH₃)₃], 32.4 [C(CH₃)₃], 31.7 [C(CH₃)₃], 26.2 [C(CH₃)₂], 23.1 [C(CH₃)₂].

[Ga₂Al(^tBu)₄H(neol)₂] (**8**). To a hexane (120 cm³) solution of [Ga₂(^tBu)₄(neol-H)₂] (0.5 g, 0.9 mmol) was added a hexane (40 cm³) solution of AlH₃(NMe₃) (0.11 g, 1.23 mmol) at room temperature. Gas was evolved immediately. The reaction was stirred for 16 hours. Yield: 0.46 g, 85%; mp 144–148 °C. MS (EI, %): *m/z* 599 (M⁺ − H, 15), 541 (M⁺ − H − ^tBu, 60), 483 (M⁺ − H − 2 ^tBu, 10), 427 (M⁺ − 3 ^tBu, 20), 369 (M⁺ − H − 4 ^tBu, 10), 183 [Ga(^tBu)₂, 25], 57 (^tBu, 100). IR (cm^{−1}): 2706 (w), 1799 (m, ν_{AlH}), 1376 (s), 1069 (s), 1022 (m), 815 (m), 720 (s). ¹H NMR (C₆D₆): δ 3.78 [4H, d, *J*(H–H) = 9.9 Hz, CH₂], 3.46 [4H, d, *J*(H–H) = 9.9 Hz, CH₂], 1.34 [18H, s, C(CH₃)₃], 1.27 [18H, s, C(CH₃)₃], 0.87 [6H, s, C(CH₃)₂], 0.72 [6H, s, C(CH₃)₂]. ¹³C

NMR (C_6D_6): δ 76.2 (OCH_2), 36.7 [$C(CH_3)_2$], 31.3 [$C(CH_3)_3$], 30.6 [$C(CH_3)_3$], 23.5 [$C(CH_3)_2$], 22.6 [$C(CH_3)_2$].

[Ga₂Al('Bu)₄Me(neol)₂] (9). To a hexane (120 cm³) solution of [Ga₂('Bu)₄(neol-H)₂] (1.0 g, 1.7 mmol) was added a hexane (50 cm³) solution of AlMe₃ (0.25 g, 3.5 mmol) at room temperature. After stirring overnight the volume was reduced *in vacuo* and the solution placed at -23°C and X-ray quality crystals were formed. Yield: 0.78 g, 75%; mp 213–216 $^\circ\text{C}$. MS (EI, %): m/z 599 ($M^+ - \text{Me}$, 34), 557 ($M^+ - ^t\text{Bu}$, 100), 485 ($M^+ - 2 ^t\text{Bu} - \text{Me}$, 10). IR (cm^{-1}): 1375 (s), 1190 (m), 1068 (br s), 1021 (m), 939 (w), 815 (m). ¹H NMR (C_6D_6): δ 3.80 [4H, d, $J(\text{H}-\text{H}) = 7.0$ Hz, CH_2], 3.40 [4H, d, $J(\text{H}-\text{H}) = 7.0$ Hz, CH_2], 1.29 [36H, s, $C(CH_3)_3$], 1.0 [6H, s, $C(CH_3)_2$], 0.57 [6H, s, $C(CH_3)_2$], -0.33 [3H, s, Al(CH_3)]. ¹³C NMR (C_6D_6): δ 76.3 (OCH_2), 36.7 [$C(CH_3)_2$], 31.7 [$C(CH_3)_3$], 30.9 [$C(CH_3)_3$], 24.4 [$C(CH_3)_2$], 22.4 [$C(CH_3)_2$].

[Ga₂Al('Bu)₅(neol)₂] (10). To a toluene (100 cm³) solution of [Ga₂('Bu)₄(neol-H)₂] (0.5 g, 0.85 mmol) was added a toluene (20 cm³) solution of Al('Bu)₃ (0.5 cm³) at room temperature. The solution was refluxed overnight. The volatiles were removed *in vacuo* and the resulting white powder was recrystallised from pentane (10 cm³) at -78°C to yield X-ray quality crystals. Yield: 0.4 g, 71%; mp 168–172 $^\circ\text{C}$. MS (EI, %): m/z 597 ($M^+ - ^t\text{Bu}$, 55), 183 [Ga('Bu)₂, 15], 57 (^tBu , 100). IR (cm^{-1}): 1400 (m), 1375 (s), 1178 (m), 1013 (s), 812 (sharp). ¹H NMR (C_6D_6): δ 4.08 [4H, d, $J(\text{H}-\text{H}) = 11.3$ Hz, CH_2], 3.32 [4H, d, $J(\text{H}-\text{H}) = 11.3$ Hz, CH_2], 1.44 [9H, s, Al($\text{C}(\text{CH}_3)_3$)], 1.36 [18H, s, GaC(CH_3)₃], 1.33 [18H, s, GaC(CH_3)₃], 1.26 [6H, s, $C(\text{CH}_3)_2$], 0.35 [6H, s, $C(\text{CH}_3)_2$]. ¹³C NMR (C_6D_6): δ 76.5 (OCH_2), 36.7 [$C(\text{CH}_3)_2$], 35.6 [$C(\text{CH}_3)_3$], 32.4 [$C(\text{CH}_3)_3$], 31.6 [$C(\text{CH}_3)_3$], 26.7 [$C(\text{CH}_3)_2$], 23.0 [$C(\text{CH}_3)_2$].

[Ga₃('Bu)₄(CH₂Ph)(neol)₂] (11). [Ga₂('Bu)₄(neol-H)₂] (0.5 g, 0.87 mmol) was dissolved in toluene (30 cm³) and refluxed overnight. The solvent was removed *in vacuo* and the solid recrystallized from hexane. Yield: 20%; mp 188–193 $^\circ\text{C}$. MS (EI, %): m/z 675 ($M^+ - ^t\text{Bu}$, 100), 641 ($M^+ - \text{CH}_2\text{Ph}$, 25), 561 ($M^+ - 3 ^t\text{Bu}$, 10), 527 ($M^+ - \text{CH}_2\text{Ph} - 3 ^t\text{Bu}$, 20), 57 (^tBu , 40). IR (cm^{-1}): 1715 (w), 1586 (m), 1400 (s), 1061 (m). ¹H NMR (C_6D_6): δ 7.35–7.0 (5H, m, C_6H_5), 3.99 [2H, d, $J(\text{H}-\text{H}) = 11.0$ Hz, CH_2], 3.85 [2H, d, $J(\text{H}-\text{H}) = 11.1$ Hz, CH_2], 3.65 [2H, dd, $J(\text{H}-\text{H}) = 11.0$ Hz, $J(\text{H}-\text{H}) = 2.0$ Hz, CH_2], 3.49 [2H, dd, $J(\text{H}-\text{H}) = 2.0$ Hz, CH_2], 2.50 (2H, s, $\text{C}_6\text{H}_5\text{CH}_2$), 1.41 [9H, s, $\text{C}(\text{CH}_3)_3$], 1.38 [9H, s, $\text{C}(\text{CH}_3)_3$], 1.32 [9H, s, $\text{C}(\text{CH}_3)_3$], 1.18 [6H, s, $\text{C}(\text{CH}_3)_2$], 1.13 [9H, s, $\text{C}(\text{CH}_3)_3$], 0.46 [6H, s, $\text{C}(\text{CH}_3)_2$]. ¹³C NMR (C_6D_6): δ 145.1, 129.1, 129.0, 128.2, 123.8 [$\text{CH}_2\text{C}_6\text{H}_5$], 78.7 (OCH_2), 77.6 (OCH_2), 37.2 [$C(\text{CH}_3)_2$], 33.0 [$C(\text{CH}_3)_3$], 32.1 [$C(\text{CH}_3)_3$], 31.4 [$C(\text{CH}_3)_3$], 31.3 [$C(\text{CH}_3)_3$], 25.1 [$C(\text{CH}_3)_2$], 22.9 [$C(\text{CH}_3)_2$].

[Ga₃Li('Bu)₆(neol)₃(OH)(THF)] (12). [Ga₂('Bu)₄(neol-H)₂] (0.6 g, 1.04 mmol) was dissolved in Et₂O (150 cm³) and was added to an Et₂O suspension of wet LiH (0.11 g, 13.7 mmol) at room temperature. The reaction was stirred for 3 days, the unreacted LiH/LiOH was removed by filtration, the Et₂O was removed *in vacuo* and resultant material redissolved in THF (30 cm³) and cooled to -23°C . Fine needle-like crystals were formed. Yield: ca. 10%. MS (EI, %): m/z 845 [$M^+ - ^t\text{Bu} - \text{THF}$]. ¹H NMR (C_6D_6): δ 3.67 (12H, s, CH_2), 1.31 [54H, s, $\text{C}(\text{CH}_3)_3$], 0.77 [18H, s, $\text{C}(\text{CH}_3)_2$].

[Ga₂Li('Bu)₄(OH)₂(neol-H)] (13). [Ga₂('Bu)₄(neol-H)₂] (0.5 g, 0.87 mmol) was dissolved in hexane (150 cm³) and a large excess of LiOH added. The reaction was stirred for 16 hours, the excess solid removed by filtration and the solution reduced to ca. 20 cm³ and placed at -23°C . Yield: ca. 30%. MS (EI, %): m/z 529 ($M^+ + \text{H}_2\text{O}$, 70), 437 ($M^+ - ^t\text{Bu} - \text{OH}$, 60), 57 (^tBu , 100). IR (cm^{-1}): 3625 (s, ν_{OH}), 1396 (m), 1338 (m), 1074 (s), 990

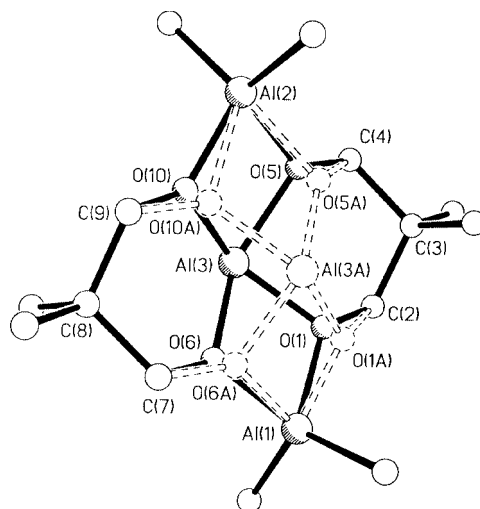


Fig. 19 View of the static disorder of the central AlO_4 core observed for $[\text{Al}_3(^t\text{Bu})_4\text{H}(\text{neol})_2]$ (**4**).

(s). ¹H NMR (C_6D_6): δ 3.58 (2H, s, CH_2), 3.17 (2H, s, CH_2), 2.76 (2H, br s, OH), 1.34 [18H, s, $\text{C}(\text{CH}_3)_3$], 1.30 [18H, s, $\text{C}(\text{CH}_3)_3$], 0.61 [6H, s, $\text{C}(\text{CH}_3)_2$]. ¹³C NMR (C_6D_6): δ 76.3 (OCH_2), 73.5 (OCH_2), 37.7 [$C(\text{CH}_3)_2$], 31.7, 31.0 [$C(\text{CH}_3)_3$], 22.3 [$C(\text{CH}_3)_2$].

[Al₃Cl₅(OSiMe₂OSiMe₂O)₂]. Hexane (30 cm³) was added to a mixture of AlCl₃ (0.3 g, 2.3 mmol) and (Me₂SiO)₄ (0.67 g, 2.3 mmol). The reaction was stirred for 6 days at room temperature. The solution was filtered to remove unreacted AlCl₃ and the hexane was removed *in vacuo*. The oily solid was recrystallised from hexane and yielded the known material. A unit cell test at room temperature confirmed the structure. $a = 11.07$ Å, $b = 13.15$ Å, $c = 18.65$ Å, $\beta = 93.34^\circ$. ¹H NMR (C_6D_6): δ 0.36 (12H, s, Si-CH₃), 0.25 (12H, s, Si-CH₃). ¹³C NMR (C_6D_6): δ 1.1 (Si-CH₃), 0.83 (Si-CH₃). MS (EI, %): m/z 571 ($M^+ - \text{Me}$, 100).

[Ga₃Cl₅(OSiMe₂OSiMe₂O)₂] (14). Prepared in an analogous manner to $[\text{Al}_3\text{Cl}_5(\text{OSiMe}_2\text{OSiMe}_2\text{O})_2]$ using GaCl₃ (0.5 g, 2.8 mmol). Yield: ca. 15%. MS (EI, %): m/z 682 ($M^+ - \text{Me}$, 100).

Crystallographic studies

Crystals of compounds **1**, **2** and **4–14** were sealed in glass capillaries under argon and mounted on one of the goniometers of an Enraf-Nonius CAD-4 (**1**), a Rigaku AFC-5S (**2**, **4–7**, **9**, **11** and **14**) or a Bruker Smart 1000 (**8**, **10**, **12** and **13**) diffractometer. Data collection was accomplished at ambient temperature in the manner previously described.¹³ The locations of most of the hydrogen atoms were obtained using SHELX-86²² and the remainder by using difference maps.²³ Disorder was noted in several cases. The most interesting example of this was a static disorder over a center of symmetry observed for many of the trimetallic species. This could be resolved for the entire molecule in compounds **7** and **10**, for the central AlO_4 core in compound **4** (see Fig. 19) and for the Al in **8**. In all cases, this disorder was symmetry derived so occurred in a 1:1 ratio. As would be expected, many of the *tert*-butyl groups were also disordered in addition to the static disorder that accompanied that described above. Dynamic disordered groups were observed in compounds **5**, **6**, **8**, **9** and **11**. With the exception of that in compound **6** (7:3) this was always in a ratio of 1:1. The thermal parameters for the THF molecule in compound **12** are very high and the molecule is located over a physically unreasonable mirror plane, but none of the positions could be resolved sensibly. Hydrogen atoms were placed in calculated positions and refined in riding models (except for the OH hydrogens in compounds **1** and **2**, and the hydride in compounds **4** and **8**, which were not found and the OH in compound **13** which was found but not refined). A summary of cell

Table 6 Summary of X-ray diffraction data

Compound	[Al ₂ (^t Bu) ₂ - (neol-H) ₂] (1)	[Ga ₂ (^t Bu) ₂ - (neol-H) ₂] (2)	[Al ₃ (^t Bu) ₄ H- (neol) ₂] (4)	[Al ₃ (^t Bu) ₄ Cl- (neol) ₂] (5)	[Al ₃ (^t Bu) ₄ Me- (neol) ₂] (6)	[Ga ₃ (^t Bu) ₅ - (neol) ₂] (7)	[Ga ₂ Al(^t Bu) ₄ H- (neol-H) ₂] (8)
Empirical formula	C ₂₆ H ₅₈ Al ₂ O ₄	C ₂₆ H ₅₈ Ga ₂ O ₄	C ₂₆ H ₅₇ Al ₃ O ₄	C ₂₆ H ₅₆ Al ₂ ClO ₄	C ₂₇ H ₅₉ Al ₃ O ₄	C ₃₀ H ₆₅ Ga ₃ O ₄	C ₂₆ H ₅₇ AlGa ₂ O ₄
<i>M_w</i>	488.71	548.13	514.66	514.66	528.68	698.98	600.14
Crystal system	Triclinic	Triclinic	Triclinic	Monoclinic	Triclinic	Triclinic	Triclinic
Space group	<i>P</i> $\bar{1}$	<i>P</i> $\bar{1}$	<i>P</i> $\bar{1}$	<i>Cc</i>	<i>P</i> $\bar{1}$	<i>P</i> $\bar{1}$	<i>P</i> $\bar{1}$
<i>a</i> /Å	9.240(1)	9.606(2)	12.793(3)	22.521(5)	10.891(2)	11.080(2)	9.303(2)
<i>b</i> /Å	9.638(2)	10.785(2)	13.708(3)	14.974(3)	10.974(2)	16.724(3)	9.721(2)
<i>c</i> /Å	10.772(4)	9.277(2)	9.721(2)	10.656(2)	15.640(3)	16.777(3)	10.799(2)
<i>a</i> °	64.94(3)	97.73(3)	98.76(3)		92.38(3)	65.38(3)	65.62(3)
<i>β</i> °	81.50(2)	111.24(3)	95.78(3)	107.76(3)	107.00(3)	82.98(3)	78.47(3)
<i>γ</i> °	68.71(1)	65.65(3)	95.78(3)		107.43(3)	82.93(3)	70.04(3)
<i>V</i> /Å ³	809.7(4)	816.0(3)	1664.0(6)	3422(1)	1688.3(6)	2804(1)	834.1(3)
<i>Z</i>	1	1	2	4	2	3	1
<i>μ</i> /cm ⁻¹	1.10	1.672	1.38	1.066	0.13	1.242	1.67
No. collected	2851	2414	4591	1655	4671	7168	3782
No. ind.	2851	2201	4353	1655	4396	7315	2363
No. obsd.	1535	1896	2803	747	3454	5284	1669
	(<i>I</i> _o) > 6.0σ(<i>I</i> _o)	(<i>I</i> _o) > 4.0σ(<i>I</i> _o)	(<i>I</i> _o) > 4.0σ(<i>I</i> _o)	(<i>I</i> _o) > 4.0σ(<i>I</i> _o)	(<i>I</i> _o) > 4.0σ(<i>I</i> _o)	(<i>I</i> _o) > 4.0σ(<i>I</i> _o)	(<i>I</i> _o) > 4.0σ(<i>I</i> _o)
<i>R</i>	0.0588	0.0431	0.087	0.077	0.050	0.0529	0.0517
<i>R_w</i>	0.0621	0.1331	0.224	0.189	0.131	0.1443	0.1307

Compound	[Ga ₂ Al(^t Bu) ₄ - Me(neol) ₂] (9)	[Ga ₂ Al(^t Bu) ₅ - (neol) ₂] (10)	[Ga ₃ (^t Bu) ₄ (CH ₂ Ph)- (neol) ₂] (11)	[Ga ₃ Li ₄ (^t Bu) ₆ (neol) ₃ - (OH)(THF)] (12)	[Ga ₂ Li(^t Bu) ₄ (OH) ₂ - (neol-H)] (13)	[Ga ₃ Cl ₅ (OSiMe ₂ - OSiMe ₂ O) ₂] (14)
Empirical formula	C ₂₇ H ₅₉ AlGa ₂ O ₄	C ₃₀ H ₆₅ AlGa ₂ O ₄	C ₃₃ H ₆₃ Ga ₃ O ₄	C ₄₃ H ₉₃ Ga ₃ Li ₄ O ₈	C ₂₁ H ₄₉ Ga ₂ LiO ₄	C ₈ H ₂₄ Cl ₅ Ga ₃ O ₆ Si ₄
<i>M_w</i>	614.16	656.24	733.00	961.22	511.98	715.04
Crystal system	Monoclinic	Triclinic	Orthorhombic	Orthorhombic	Monoclinic	Monoclinic
Space group	<i>C2/c</i>	<i>P</i> $\bar{1}$	<i>P2₁2₁2₁</i>	<i>P2₁2₁2₁</i>	<i>P2₁/c</i>	<i>P2₁/n</i>
<i>a</i> /Å	22.713(5)	11.048(2)	20.697(4)	10.658(2)	14.550(3)	11.146(2)
<i>b</i> /Å	15.161(3)	16.692(3)	17.050(3)	21.256(4)	17.041(3)	13.156(3)
<i>c</i> /Å	10.610(2)	16.796(3)	10.878(2)	27.919(6)	11.756(2)	18.775(4)
<i>a</i> °		65.35(3)				
<i>β</i> °	108.21(3)	88.41(3)			102.23(3)	93.11(3)
<i>γ</i> °		82.81(3)				
<i>V</i> /Å ³	3471(1)	2792(1)	3838(1)	6325(2)	2848(1)	2749.1(9)
<i>Z</i>	4	3	4	4	4	4
<i>μ</i> /cm ⁻¹	1.60	0.1498	0.212	1.30	1.91	1.90
No. collected	4656	12847	3060	20813	12864	4173
No. ind.	2273	8009	3028	8630	4098	3956
No. obsd	1398	4255	2093	1975	2096	2633
	(<i>I</i> _o) > 4.0σ(<i>I</i> _o)	(<i>I</i> _o) > 4.0σ(<i>I</i> _o)	(<i>I</i> _o) > 4.0σ(<i>I</i> _o)	(<i>I</i> _o) > 4.0σ(<i>I</i> _o)	(<i>I</i> _o) > 4.0σ(<i>I</i> _o)	(<i>I</i> _o) > 4.0σ(<i>I</i> _o)
<i>R</i>	0.0543	0.0688	0.056	0.0817	0.054	0.104
<i>R_w</i>	0.134	0.1742	0.132	0.1703	0.116	0.130

parameters, data collection and structure solution is given in Table 6. Scattering factors were taken from ref. 24.

CCDC reference number 186/1959.

Acknowledgements

Financial support for this work is provided by the Robert A. Welch Foundation, the Office of Naval Research and the National Science Foundation. The Bruker CCD Smart System Diffractometer was funded by the Robert A. Welch Foundation and the Bruker Avance 200 NMR spectrometer was purchased with funds from ONR Grant N00014-96-1-1146. A. R. B. acknowledges the support of the Alexander von Humboldt Foundation for a Senior Scientist Fellowship and Professor H. W. Roesky for his support, hospitality and useful scientific discussion.

References

- C. E. Holloway and M. Melnik, *J. Organomet. Chem.*, 1977, **543**, 1.
- (a) A. Von Grosse and J. M. Mavity, *J. Org. Chem.*, 1940, **5**, 106; (b) J. H. Rogers, A. W. Apblett, W. M. Cleaver, A. N. Tyler and A. R. Barron, *J. Chem. Soc., Dalton Trans.*, 1992, 3179.
- (a) S. Pasynkiewicz and W. Ziemkowska, *J. Organomet. Chem.*, 1992, **423**, 1; (b) S. Pasynkiewicz and W. Ziemkowska, *J. Organomet. Chem.*, 1992, **437**, 99; (c) W. Ziemkowska, S. Pasynkiewicz and T. Glowiak, *J. Organomet. Chem.*, 1998, **562**, 3; (d) W. Ziemkowska, S. Pasynkiewicz and T. Skrok, *Main Group Metal Chem.*, 1998, **21**, 105.
- W. Ziemkowska and S. Pasynkiewicz, *J. Organomet. Chem.*, 1996, **508**, 243.
- (a) D. A. Atwood and D. Rutherford, *Comments Inorg. Chem.*, 1996, **19**, 25; (b) J. A. Jegier, M. Muñoz-Hernández and D. A. Atwood, *J. Chem. Soc., Dalton Trans.*, 1999, 2583 and references therein.
- C. N. McMahon, L. Alemany, R. L. Callender, S. G. Bott and A. R. Barron, *Chem. Mater.*, 1999, **11**, 795.
- A. Haaland, *Coordination Chemistry of Aluminum*, ed. G. H. Robinson, VCH, New York, 1993, ch. 1.
- C. N. McMahon, S. G. Bott and A. R. Barron, *J. Chem. Soc., Dalton Trans.*, 1997, 3129.
- (a) R. D. G. Jones, *Acta Crystallogr., Sect. B*, 1976, **32**, 301; (b) T. Sugawara, T. Mochida, A. Miyazaki, A. Izuoka, N. Sato, Y. Sugawara, K. Deguchi, Y. Moritomo and Y. Tokura, *Solid State Chem.*, 1992, **83**, 665.
- (a) D. G. Hodgson, *Prog. Inorg. Chem.*, 1975, **19**, 173; (b) C. M. Harris and E. Sinn, *Coord. Chem. Rev.*, 1969, **4**, 391; (c) S. Yamada, *Coord. Chem. Rev.*, 1966, **1**, 415.
- J. K. Ruff and M. F. Hawthorne, *J. Am. Chem. Soc.*, 1960, **82**, 2141.
- (a) B. Neumuller and F. Gahlmann, *Z. Anorg. Allg. Chem.*, 1992, **612**, 123; (b) B. Neumuller and F. Gahlmann, *Chem. Ber.*, 1992, **126**, 1579; (c) T. Krauter, B. Werner and B. Neumuller, *Z. Naturforsch., Teil B*, 1996, **51**, 637; (d) M. R. Kopp and B. Neumuller, *Z. Anorg. Allg. Chem.*, 1997, **623**, 769.

- 13 M. B. Power, S. G. Bott, J. L. Atwood and A. R. Barron, *J. Am. Chem. Soc.*, 1990, **112**, 3446.
- 14 (a) M. R. Mason, J. M. Smith, S. G. Bott and A. R. Barron, *J. Am. Chem. Soc.*, 1993, **115**, 4971; (b) Y. Koide, J. A. Francis, S. G. Bott and A. R. Barron, *Polyhedron*, 1998, **17**, 983.
- 15 (a) G. C. Pimentel and A. L. McClellan, *The Hydrogen Bond*, Freeman, San Francisco, 1960; (b) M. D. Joesten and L. J. Schaad, *Hydrogen Bonding*, Dekker, New York, 1974.
- 16 V. E. Shklover, Yu. T. Struchkov, M. M. Levitskii and A. A. Zhdanov, *Zh. Strukt. Khim.*, 1986, **27**, 120.
- 17 (a) M. Bonamico, *Chem. Commun.*, 1966, 135; (b) M. Bonamico and G. Dessy, *J. Chem. Soc. A*, 1968, 291.
- 18 See for example, (a) M. B. Hursthouse and Md. A. Hossain, *Polyhedron*, 1984, **3**, 95; (b) M. B. Hursthouse, M. Motevalli, M. Sanganee and A. Sullivan, *J. Chem. Soc., Chem. Commun.*, 1991, 1709; (c) M. Motevalli, M. Sanganee, P. D. Savage, S. Shah and A. Sullivan, *J. Chem. Soc., Chem. Commun.*, 1993, 1132.
- 19 (a) A. Almemmingen, O. Bastiansen, V. Ewing, K. Hedberg and M. Traetteberg, *Acta Chem. Scand.*, 1963, **17**, 2455; (b) W. Airey, C. Glidwell, D. W. H. Rankin, A. G. Robiette, G. M. Sheldrick and D. W. Cruickshank, *Trans. Faraday Soc.*, 1970, **66**, 551; (c) W. Airey, C. Glidwell, A. G. Robiette and G. M. Sheldrick, *J. Mol. Struct.*, 1971, **8**, 423; (d) B. Morosin and L. A. Harrah, *Acta Crystallogr., Sect. B*, 1981, **37**, 579.
- 20 (a) W. Uhl, *Z. Anorg. Allg. Chem.*, 1989, **570**, 37; (b) H. Lehmkuhl, O. Olbrysch and H. Nehl, *Liebigs Ann. Chem.*, 1973, 708; (c) H. Lehmkuhl and O. Olbrysch, *Liebigs Ann. Chem.*, 1973, 715.
- 21 R. A. Kovar, H. Derr, D. Brandau and J. O. Callaway, *Inorg. Chem.*, 1975, **14**, 2809.
- 22 G. M. Sheldrick, *Acta Crystallogr., Sect. A*, 1990, **46**, 467.
- 23 M. C. Burla, M. Carnalli, G. Cascarano, C. Giacovazzo, G. Polidori, R. Spagna and D. Viterbo, *J. Appl. Crystallogr.*, 1989, **22**, 389.
- 24 *International Tables for X-ray Crystallography*, Kynoch Press, Birmingham, 1974, vol. IV, pp. 99, 149.